TELKOMNIKA Indonesian Journal of Electrical Engineering
Vol.12, No.5, May 2014, pp. 3560 ~ 3569
DOI: http://dx.doi.org/10.11591/telkomnika.v12i5.3999

A Convenient Control Strategy of Bearingless Induction Motor Based on Inverse System Method

Wen-shao Bu*, Chun-xiao Lu, Cong-lin Zu
College of Information Engineering, Henan University of Science and Technology,
Luoyang, 471023, China
*Corresponding author, e-mail: wsbu@163.com

Abstract

To achieve the reliable control of bearingless induction motor which is a multi-variable and nonlinear object, a convenient decoupling control strategy based on inverse system method is proposed. The reversibility of four-pole torque system was analyzed, and the inverse system models were analysed also. Then the torque system was decoupled into two second-order linear subsystems: one is the rotor speed system; another is the rotor flux system. The suspension control system adopts negative feedback control strategy, and the required air-gap flux linkage of torque system was obtained from the rotor flux and stator current ontime; finally, synthesis and simulation of the decoupling control system for bearingless induction motor were researched. Simulation results have demonstrated that good performance can be achieved. The presented control strategy is feasible.

Keywords: *bearingless induction motor, reversibility analyse, convenient control strategy, decoupling control system, synthesis and simulation*

1. Introduction

Based on the similarity of magnetic bearing and usual motor's stator, Bearingless motor is proposed [1-5]. Bearingless motor is a newly type of electric machine with suspension control windings embedded in the stator slots along with the conventional motor windings. In bearingless motor, the usual motor windings are called torque windings, witch will produce usual torque magnetic field; and the suspension control windings will produce suspension magnetic field. By the interaction between torque magnetic field and suspension magnetic field, the radial suspension force will come into being [1], [6-7]. Because of the structure complexity, the mathematical model of bearingless motor is so complex; there are cross-couplings between multi-variables. In order to achieve good control performance of bearingless motor, it is necessary to achieve the decoupling between relevant variables. The inverse system method is an effective decoupling measure for multi-variable and nonlinear system, and its basic idea can be described as following: based on the original system model, the inverse system can be constructed, and the inverse system can be used to compensate the original system into several decoupled linear subsystem [8].

In the paper, the inverse system method will be applied to the variable frequency speed adjustment system of three-phase bearingless induction motor. The reversibility of four-pole torque system was analyzed based on rotor flux orientation, and the inverse system method was analyzed also. Then the torque system will be decoupled into two second-order linear subsystems: one is the rotor speed subsystem; another is the rotor flux subsystem; for convenience, the suspension control system will adopt negative feedback control strategy, and the required air-gap flux linkage of torque system will be calculated online from the rotor flux and stator current of torque system.

2. Mathematical Model of Bearingless Induction Motors

2.1. Working Principle of Bearingless Induction Motor

Bearingless induction motor is a newly type of electric machine that there are two sets of windings with a difference in pole-pair numbers embedded together in its stator slots: torque windings (with pole pair p_1 and angular frequency ω_1), and suspension control windings (with

Received July 24, 2013; Revised December 15, 2013; Accepted January 4, 2014

pole pair p_2 and angular frequency ω_2). Relevant researche results show that only when two sets of windings meet the qualification of "$p_2 = p_1 \pm 1$, $\omega_1 = \omega_2$", and the two sets of magnetic fields produced by two sets of windings rotate in the same direction, can the radial force that can be stably controllable be produced [1], [8-10]. By the interaction between torque magnetic field and suspension magnetic field, the distribution of composite magnetic field in air-gap was changed, then a radial force generates pointing to the direction of the magnetic field enhancement, thus the stable suspension of the rotor shaft is achieved.

In the paper, bearingless induction motors combined 4-pole torque windings and 2-pole suspension control windings are selected as the object for study. Figure 1 shows the principle of the magnetic suspension force generation for an induction-type bearingless motor. When torque windings and suspension control windings are electrified by I_1, I_2, they will generate 4-pole flux linkage ψ_1 and 2-pole flux linkage ψ_2. Here, α and β represent the axis for rotor displacement control. At no-load situation, if the suspension control windings are electrified the current I_2 in the direction as shown in Figure 1, on the upper of air gap, the air gap flux linkage density would be increase because of ψ_1 and ψ_2 in the area pointing to the same direction. But on the lower side, the flux linkage density decreases for ψ_2 being in the opposite direction with ψ_1. Therefore, the radial electromagnetic force F_β is generated along β-direction due to the imbalance of magnetic field. The radial force in the opposite β-direction would be produced when suspension control windings are electrified the current which contrary to I_2 in Figure1. In the same way, the radial force along α-direction can be generated also.

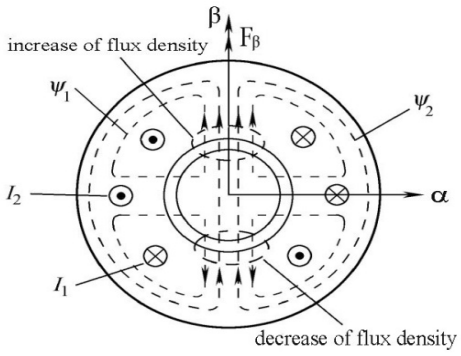

Figure 1. Principle of Magnetic Suspension Force Generation of Bearingless Induction Motor

2.2. Mathematical Models of Four-pole Torque System

The principle of torque generation for bearingless induction motor is similar with the conventional induction motor. The mathematical model of torque system consists three parts in d-q coordinate, which is voltage equations, flux linkage equations and torque equations. Voltage equations are shown as Equation (1).

$$\left.\begin{aligned} U_{s1d} &= R_{s1} i_{s1d} + p\psi_{s1d} - \omega_1 \psi_{s1q} \\ U_{s1q} &= R_{s1} i_{s1q} + p\psi_{s1q} + \omega_1 \psi_{s1d} \\ U_{r1d} &= R_{r1} i_{r1d} + p\psi_{r1d} - \omega_s \psi_{r1q} = 0 \\ U_{r1q} &= R_{r1} i_{r1q} + p\psi_{r1q} + \omega_s \psi_{r1d} = 0 \end{aligned}\right\} \quad (1)$$

Where ω_1 is the rotation angular speed of the d-q sysnchronous reference frame; ω_s is the slip angle frequency, $\omega_s = \omega_1 - \omega$; ω is the angular speed of the rotor; i_{s1d}、i_{s1q} and i_{r1d}、i_{r1q} are the stator current component and the rotor current component of the torque windings in d-q reference frame; U_{s1d}、U_{s1q} and U_{r1d}、U_{r1q} are the stator voltage component and the rotor voltage component of the torque windings in d-q reference frame; ψ_{s1d}、ψ_{s1q} and ψ_{r1d}、ψ_{r1q} are the component of the stator flux linkage and the rotor flux linkage of the torque windings in d-q reference frame; R_{s1}、R_{r1} are the stator and rotor resistance; p is the differential operator.

Equation (2) shows the rotor flux linkage equation.

$$\left.\begin{aligned}\psi_{s1d} &= L_s i_{s1d} + L_m i_{r1d} = \psi_{1d} + L_{s1} i_{s1d} \\ \psi_{s1q} &= L_s i_{s1q} + L_m i_{r1q} = \psi_{1q} + L_{s1} i_{s1q} \\ \psi_{r1d} &= L_m i_{s1d} + L_r i_{r1d} = \psi_{1d} + L_{rl} i_{r1d} \\ \psi_{r1q} &= L_m i_{s1q} + L_r i_{r1q} = \psi_{1q} + L_{rl} i_{r1q}\end{aligned}\right\} \quad (2)$$

In Equation (2): ψ_{1d}、ψ_{1q} are the air gap flux component of the torque windings in d-q reference frame; L_m is the mutual induction between stator and rotor in d-q reference frame; L_s is the self-induction of the stator, $L_s=L_m+L_{sl;}$ L_s is the self-induction of the rotor, $L_r=L_m+L_{rl}$; L_{sl}、L_{rl} are the leakage induction of the stator and the rotor.

Equation (3) shows the Torque equation.

$$T_e = p_1 \frac{L_m}{L_r}(\psi_{r1d} i_{s1q} - \psi_{r1q} i_{s1d}) \quad (3)$$

Where, p_1 is the pole-pairs of the torque windings.

2.3. Mathematical Models of Two-pole Suspension System

The radial magnetic suspension forces of the bearingless motor can be expressed as following [9, 10]:

$$F_\alpha = K_m(i_{s2d}\psi_{1d} + i_{s2q}\psi_{1q}), \quad F_\beta = K_m(i_{s2d}\psi_{1q} - i_{s2q}\psi_{1d}) \quad (4)$$

Where K_m is the levitation force coefficient that is related to the structure of the motor.

In addition, there is an eccentric magnetic pull on the rotor that can be written as:

$$F_{s\alpha} = K_s\alpha, \quad F_{s\beta} = K_s\beta \quad (5)$$

Where K_s is the radial displacement coefficient.

2.4. Motion Equation of the Bearingless Motor

The motion equations of the bearingless motor can be expressed as Equation (6).

$$\left.\begin{aligned} m\ddot{\alpha} &= F_\alpha - F_{s\alpha} \\ m\ddot{\beta} &= F_\beta - F_{s\beta} \\ J\dot{\omega}_r / p_1 &= T_e - T_L\end{aligned}\right\} \quad (6)$$

Where, m is the rotor mass; α and β are the eccentric displacements of rotor from the stator center.

3. Inverse Decoupling Control of the Torque System

3.1. State Equations of the Torque System

Oriented the d-axes in the rotor flux linkage, then $\psi_{r1}=\psi_{r1d}$, $\psi_{r1q}=\dot{\psi}_{r1q}=0$. Then, Substituting Equation (2) into Equation (1), and eliminating i_{r1d}、i_{r1q}、ψ_{r1d}、ψ_{r1q}, and the state equations of the torque system can be written as [11]:

$$\frac{di_{s1d}}{dt} = -\frac{R_s L_r^2 + R_r L_m^2}{\sigma L_s L_r^2} i_{s1d} + \omega_1 i_{s1q} + \frac{L_m}{\sigma L_s L_r T_r}\psi_{r1} + \frac{1}{\sigma L_s} u_{s1d} \quad (7)$$

$$\frac{di_{s1q}}{dt} = -\omega_1 i_{s1d} - \frac{R_s L_r^2 + R_r L_m^2}{\sigma L_s L_r^2} i_{s1q} - \frac{L_m}{\sigma L_s L_r} \omega \psi_{r1} + \frac{1}{\sigma L_s} u_{s1q} \tag{8}$$

$$\frac{d\psi_{r1}}{dt} = -\frac{1}{T_r} \psi_{r1} + \frac{L_m}{T_r} i_{s1d} \tag{9}$$

$$\frac{d\omega}{dt} = \frac{p_1^2 L_m}{J L_r} \psi_{r1} i_{s1q} - \frac{p_1}{J} T_L \tag{10}$$

In addition, there is following relation equation:

$$\dot{\psi}_{r1q} = -(\omega_1 - \omega_r)\psi_{r1} + L_{m1} i_{s1q} / T_r = 0 \tag{11}$$

Then the rotation angular speed of the d-q reference frame can be written as following:

$$\omega_1 = \omega + \frac{L_{m1} i_{s1q}}{T_r \psi_{r1}} \tag{12}$$

By the Equation (9), the rotor flux linkage can be deduced as:

$$\psi_r = \frac{L_{m1}}{T_r s + 1} i_{s1d} \tag{13}$$

According to the Equation (12), the rotation angle of the rotor flux linkage can be deduced as the following:

$$\varphi = \int \omega_1 = \int (\omega_r + \omega_s) dt = \int [\omega_r + L_{m1} i_{s1q} / (T_r \psi_r)] dt \tag{14}$$

3.2. Reversibility Analysis of the Torque Systems

The state variables are chosen as [12-15]:

$$x = (x_1, x_2, x_3, x_4)^T = (i_{s1d}, i_{s1q}, \psi_r, \omega)^T \tag{15}$$

Input variables are chosen as:

$$u = (u_1, u_2)^T = (u_{s1d}, u_{s1q})^T \tag{16}$$

Output variables are chosen as:

$$y = (y_1, y_2)^T = (x_3, x_4)^T = (\psi_r, \omega)^T \tag{17}$$

The state equation of the system can be written as:

$$\left.\begin{aligned} \dot{x}_1 &= -(\gamma - \tau)x_1 + (x_4 + L_m \delta x_2 / x_3)x_2 + \delta \tau \eta x_3 + \delta u_1 \\ \dot{x}_2 &= -(\gamma - \tau)x_2 - (x_4 + L_m \delta x_2 / x_3)x_1 - \delta \eta x_3 x_4 + \delta u_2 \\ \dot{x}_3 &= L_m \tau x_1 - \tau x_3 \\ \dot{x}_4 &= \mu x_2 x_3 - \frac{p_1}{J} T_L \end{aligned}\right\} \tag{18}$$

In equation (18):

$$\sigma = 1 - \frac{L_m^2}{L_s L_r},\ \gamma = \frac{R_s}{\sigma L_s} + \frac{R_r}{\sigma L_r},\quad \tau = \frac{R_r}{L_r},\ \delta = \frac{1}{\sigma L_s},\ \mu = \frac{p_1^2 L_m}{J L_r},\quad \eta = \frac{L_m}{L_r}$$

In order to analysis the reversibility of the system, interactor algorithm is adopted. Calculate the derivative of the output $y = (y_1, y_2)^T$ with respect to time, until the Input variables are revealed. The calculation procedures can be expressed as following:

$$\left.\begin{aligned} \dot{y}_1 &= L_m \tau x_1 - \tau x_3 \\ \ddot{y}_1 &= L_m \tau[-(\gamma-\tau)x_1 + (x_4 + L_m \tau x_2 / x_3)x_2 + \delta\tau\eta x_3 + \delta u_1] - \tau^2 \\ \dot{y}_2 &= \mu x_2 x_3 - \frac{p_1}{J} T_L \\ \ddot{y}_2 &= \mu x_3[-(\gamma-\tau)x_2 - (x_4 + L_m \tau x_2 / x_3)x_1 - \delta\eta x_3 x_4 + \delta u_2] + \mu\tau x_2 (L_m x_1 - x_3) \end{aligned}\right\} \quad (19)$$

Assuming $Y = (\ddot{y}_1, \ddot{y}_2)$, then the Jacobi matrix with respect to input variable can be expressed as following:

$$A = \frac{\partial Y}{\partial u} = \begin{pmatrix} \frac{L_m \tau}{L_s \sigma} & 0 \\ 0 & \frac{\mu x_3}{L_s \sigma} \end{pmatrix} \quad (20)$$

$x_3 = \psi_{r1} \neq 0$, $\det(A) = L_m \tau \mu x_3 / L_s^2 \sigma^2 \neq 0$, $rank(A) = 2 < 4$. The relative order of the system is $\alpha = (\alpha_1, \alpha_2)^T = (2,2)^T$. It is easily obtained that $\alpha_1 + \alpha_2 = 4$, which is equal to the order of the system. Then, there is conclusion that the system is reversible.

Assuming $Y = (\ddot{y}_1, \ddot{y}_2)^T = (v_1, v_2)^T$, and substituting it into Equation (19) and (20), then the inverse system model of four-pole torque system can be written as:

$$\left.\begin{aligned} u_1 &= \frac{1}{\delta}\left[\frac{1}{L_m \tau} v_1 + \gamma x_1 - \tau\left(\delta\eta + \frac{1}{L_m}\right)x_3 - \left(x_4 + \frac{L_m \tau x_2}{x_3}\right)x_2\right] \\ u_2 &= \frac{1}{\delta}\left[\frac{1}{\mu x_3} v_2 + \gamma x_2 + x_1 x_4 + \delta\eta x_3 x_4\right] \end{aligned}\right\} \quad (21)$$

Where v_1、v_2 are input variables of the inverse system.

Connecting the inverse system in front of the torque system in series, and complexing them together, then the torque system is decoupled to two pseudo-linear subsystems.

The input-output relations of the compound system can be expressed as following:

$$\ddot{y}_1 = v_1,\ \ \ddot{y}_2 = v_2 \quad (22)$$

Where: $y_1 = \psi_{r1}$, $y_2 = \omega$.

4. Negative Feedback Control of the Suspension System

It can be seen from Equation (4) that the radial suspension force is generated by the interaction between the air gap flux linkage of torque windings and the stator current of suspension control windings. In order to achieve the decoupling control between radial

suspension force components, the amplitude of air gap flux linkage is need to be identified accurately so that the suspension control current can be calculated according to the required magnetic suspension force.

The amplitude of air gap flux linkage can be identified by the relationship between air gap flux linkage and rotor flux linkage, as Equation (23) and (24).

$$\psi_{1d} = \frac{L_m}{L_r}(\psi_{r1} + L_{rl} i_{s1d}) \tag{23}$$

$$\psi_{1q} = \frac{L_m}{L_r} L_{rl} i_{s1q} \tag{24}$$

Then the required suspension control current can be deduced by Equation (4) as following:

$$\begin{pmatrix} i_{s2d} \\ i_{s2q} \end{pmatrix} = \frac{1}{K_m(\psi_{1d}^2 + \psi_{1q}^2)} \begin{pmatrix} \psi_{1d} & \psi_{1q} \\ \psi_{1q} & -\psi_{1d} \end{pmatrix} \begin{pmatrix} F_\alpha \\ F_\beta \end{pmatrix} \tag{25}$$

And Equation (25) can be rewritten as Equation (26) as well.

$$\begin{pmatrix} i_{s2d} \\ i_{s2q} \end{pmatrix} = \frac{1}{K_{m1}} \begin{pmatrix} \cos\rho & \sin\rho \\ \sin\rho & -\cos\rho \end{pmatrix} \begin{pmatrix} F_\alpha \\ F_\beta \end{pmatrix} \tag{26}$$

In Equation (25) and (26):

$$K_{m1} = K_m(\psi_{1d}^2 + \psi_{1q}^2), \quad \rho = \arctan\left(\psi_{1q} / \psi_{1d}\right) \tag{27}$$

5. Synthesizing System

5.1. Closed Loop Controllers Design

From the inverse system compensation, the torque system is decoupled into two second-order linear subsystems: one is the rotor speed subsystem; the other is the rotor flux subsystem, each of them can be controlled by v_1, v_2 independently, as shown in Figure 2. But in practice, under the effect of all kinds of factors, the pseudo-linear system that has decoupled by inverse system is not a simple and ideal linear system, thus closed loop controller is needed to design according to linear system theory to improve the dynamic and static performance and anti-jamming capability for the whole control system. As a kind of classic and effective controller, PID controllers are suitable for the pseudo-linear system of bearingless induction motor.

In the paper, for the transfer functions of motor speed subsystem and rotor flux subsystem can be expressed with $G(s) = 1/s^2$, PD controllers are used to synthesizing the torque system. The transfer function of PD controller can be written as:

$$G_c(s) = K_p + K_d s = K_p(1 + T_d s) \tag{28}$$

In Equation (28), K_p is the proportional gain coefficient, K_d is the differential gain coefficient, T_d is differential time constant, which can be shown as follows:

$$T_d = \frac{K_d}{K_p} \tag{29}$$

The open loop transfer function of the second-ordered system with PD controller is:

$$G_{ol}(s) = \frac{K_p + K_d s}{s^2} = \frac{K_p(1+T_d s)}{s^2} \tag{30}$$

The parameters of the speed controller and the rotor flux controller are the same; the setting of the parameters can be determined by method of frequency domain analysis. In the paper, K_p =1000, K_d =50 were finally selected as parameter for the controllers. Then the open loop transfer function of the system is:

$$G_{ol}(s) = \frac{50(s+20)}{s^2} \tag{31}$$

The closed loop transfer function of the system can be written as:

$$G_{cl} = \frac{50(s+20)}{s^2+50s+1000} \tag{32}$$

For the suspension control system, negative feedback control is used after the identification of air gap flux linkage. The structure of the suspension control system is simple relatively, the traditional PID controllers are appropriate to synthesizing for a good performance.

5.2. Overall Structure of Control System and Simulation Results

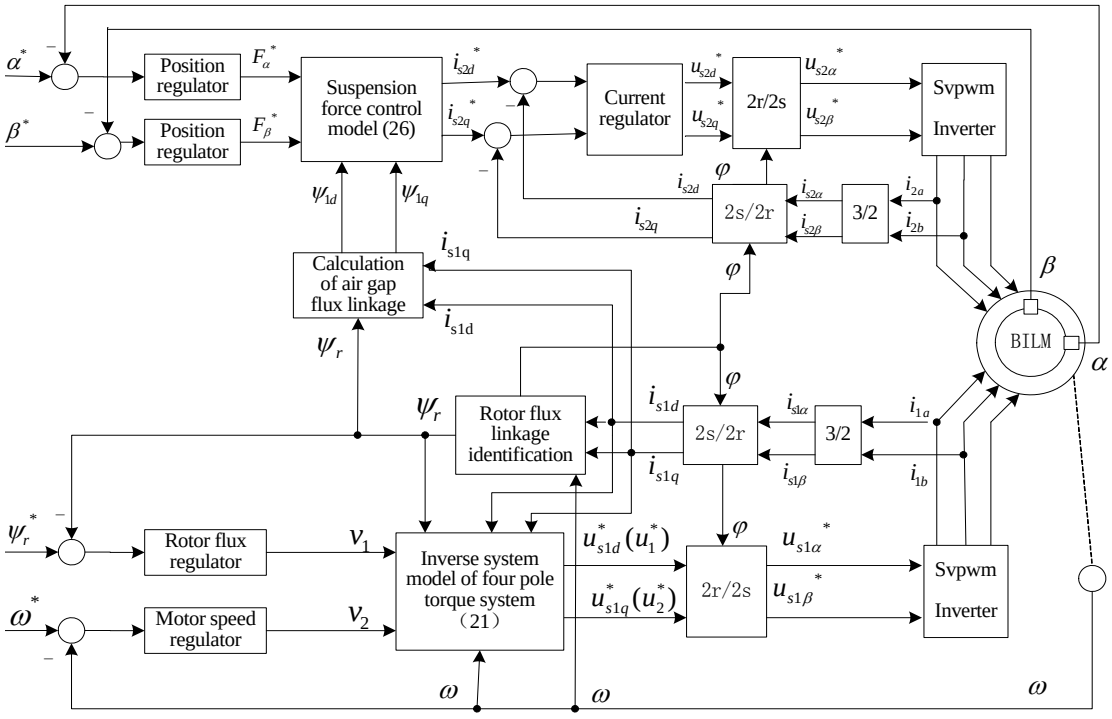

Figure 2. Control system of bearingless induction motor based on inverse system

The designed overall construct of control system for bearingless induction motor is shown as Figure 2. The stator currents and radial displacements can be measured directly; the motor speed can be recognized by speed sensorless; the rotor flux linkage and the air gap flux linkage can be identified by flux observer, the rotation angular speed can be derived from Equation (12). As shown in Figure 2, for the torque system, the detected speed and rotor flux linkage are compared with their given values, the deviation values are the input of inverse system v_1, v_2. The outputs of inverse system, i.e. u^*_{s1d} and u^*_{s1q} are transformed to $u^*_{s1\alpha}$and $u^*_{s1\beta}$. Then by SVPWM inverter, the torque control of three-phase bearingless induction motor can be

achieved. For the suspension control system, the difference between the actual radial displacements α, β and their given values are regulated by PID controller, the required given values of radial suspension force are derived. The current components i^*_{s2d}, i^*_{s2q} for suspension control can be deduced by Equation (26). By current regulating, u^*_{s2d}, u^*_{s2q} are obtained, and by coordinate transformation, $u^*_{s2\alpha}$, $u^*_{s2\beta}$ are derived witch will be used as the reference voltages of SVPWM modulation.

In order to verify the feasibility of the proposed decoupling control method as shown in Figure 3, simulation is implemented based on Matlab/Simulink, the bearingless induction motor with two-pole suspension winding and four-pole torque winding is adopted as the control object . The motor parameters are given as followings: the stator resistance R_s=0.435Ω, the rotor resistance R_r=0.816Ω, the self-inductance of stator L_s=0.071H, the self-inductance of rotor L_r=0.071H, the mutual inductance of stator and rotor L_m=0.069H, the rotor moment of inertia J=0.189kg·m^2, the touch down bearing clearance δ=250μm, the mass of rotor m=3.25kg, the radial displacement coefficient K_s=2.3H/m.

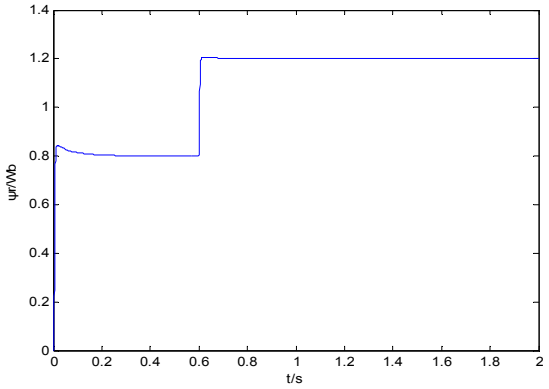

Figure 3. Rotor Flux Linkage Response Waveform

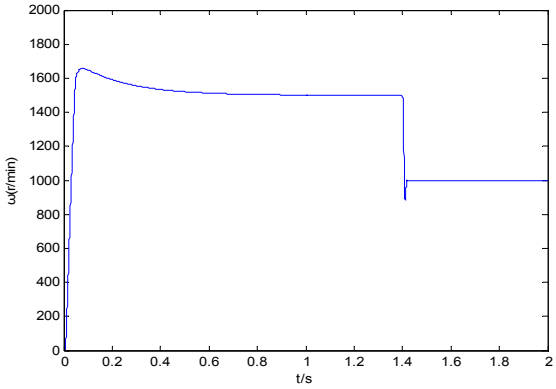

Figure 4. Rotor Speed Response Waveform

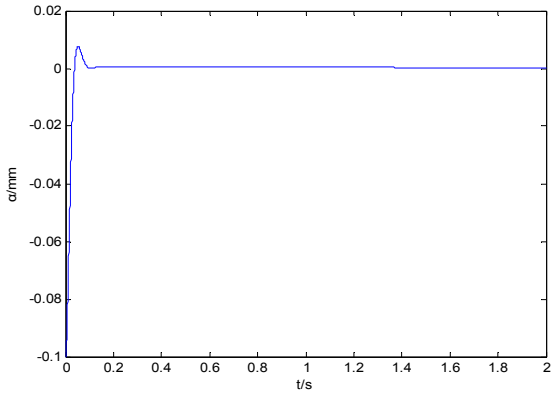

Figure 5. Response Waveform of α-direction Radial Displacement

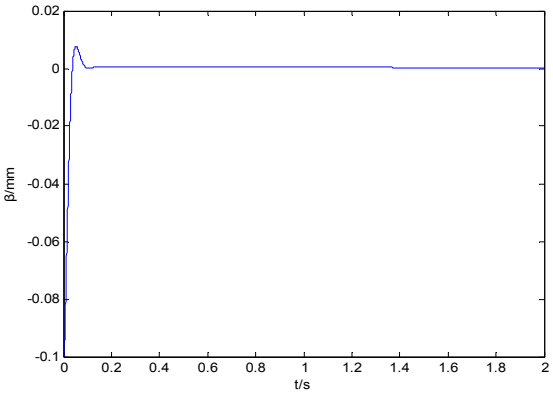

Figure 6. Response Waveform of β-direction Radial Displacement

In the simulation experiment, the initial values are set as followings: the given value of rotor speed is 1500r/min, the given value of rotor flux linkage is 0.8Wb; the initial values of two radial displacements are -0.1mm, and the given values of radial displacements are 0.0mm; the motor will start with no load. The simulation results of the decoupoling control system are shown as Figure 3 to Figure 6. From the simulation results, we can see that each of the output meets the given value with fast response times and small overshoot. In order to verify the effectiveness of the decoupling control strategy, the given signal of the system varies with time. At t=0.6s, the

given value of rotor flux linkage be changed to 1.2Wb; at t=1.4s, the given value of rotor speed be changed to 1000r/min. As shown in Figure 4 to Figure 7, the variation of rotor speed couldn't affect the rotor flux linkage and the radial displacements, and the variation of the rotor flux linkage has no influence on the other controlled variables also.

To further verify the effects of decoupling control of suspension control system, the given value of α-direction radial displacement be changend to 0.02mm at the moment of 0.5s; at the moment of 1.2s, the given value returned to 0; at the moment of 0.8s, the given value of β-direction displacement be changed to -0.02mm, and at the moment of 1.5s, the given value of β-direction displacement returns to 0.0mm. Fig.8 shows the simulation results. As shown in Figure 7, when one of the radial displacement components changes, another is not be impacted.

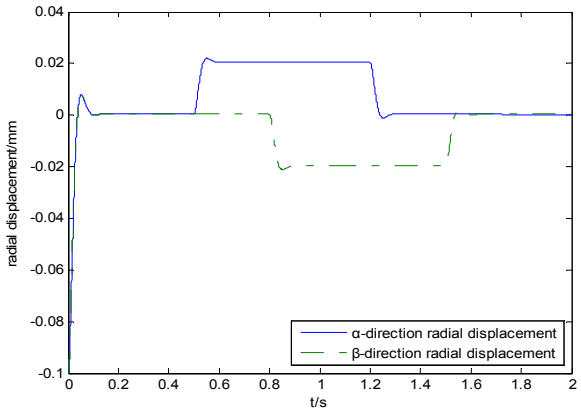

Figure 7. Decoupling Control Response Waveforms of Suspension System

From above simulation results, better decoupling control performance of bearingless induction motor has achieved, and the proposed decoupling control strategy is effective.

6. Conclusion

Three-phase bearingless induction motor is a multi-variable, nonlinear and strong-coupling object. Aiming at the the strong-coupling problem of Bearingless induction motor, the paper proposed a convenient inverse system decoupling control strategy. By compensation of the Inverse system, the four-pole torque system is decoupled into two second-order linear integral subsystems: one is the rotor speed system; another is the rotor flux subsystem. Then, using the rotor flux linkage and stator current, the required air-gap flux linkage of torque system is identified ontime. By linear feedback control, the radial displacements can be control reliably.

Simulation results have demonstrated that good decoupling control performance can be achieved with the presented control strategy; the overall system has fine dynamic and static performance and higher anti-jamming capability. The given control strategy is feasible and effective.

Acknowledgements

The supports of National Natural Science Foundation of China (51277053), International Cooperation Project on Science and Technology of Henan Province (114300510029), and Nature Science Fund of Henan Province Education Bureau (2010B510011), are acknowledged.

References

[1] A Chiba, T Fukao, O Ichikawa, et al. Magnetic bearings and bearingless drives. Boston, MA: Elsevier Newnes Press. 2005.

[2] Junichi Asama, Yuki Hamasaki, Takaaki Oiwa, et al. Proposal and Analysis of a Novel Single-Drive Bearingless Motor. *IEEE Transactions on Industrial Electronics*. 2013; 60(1): 129-138.
[3] Valci F Victor, Filipe O Quintaes , José SB Lopes, et al. Analysis and Study of a Bearingless AC Motor Type Divided Winding Based on a Conventional Squirrel Cage Induction Motor. *IEEE Transactions on Magnetics*. 2012; 48(11): 3571-3574.
[4] WS Bu, SH Huang, SM Wan, et al. General Analytical Models of Inductance Matrices of Four-Pole Bearingless Motors with Two-Pole Controlling Windings. *IEEE Transactions on Magnetics*. 2009; 45(9): 3316-3321.
[5] A Chiba, JA Santisteban. A PWM Harmonics Elimination Method in Simultaneous Estimation of Magnetic Field and Displacements in Bearingless Induction Motors. *IEEE Transactions on Industry Applications*. 2012; 48(1): 124-131.
[6] A Chiba, J Asama. Influence of Rotor Skew in Induction Type Bearingless Motor. *IEEE Transactions on Magnetics*. 2012; 48(11): 4646-4649.
[7] Wenshao Bu, Shaojie Wang, Shenghua Huang. Decoupling control system of three-phase bearingless induction motor. *Electric Machines and Control.* 2011; 15(12): 32-37, 4.
[8] Xianzhong Dai, He Dan, et al. MIMO system inveritibility and decoupling control strategies based on ANN α-order inversion. *IEE Trans. on Control theory and Appl*. 2001; 148(2): 125-236.
[9] Heng Nian, Yikang He. *Analytical modeling and feedback control of the magnetic levitation force for an induction type bearingless motor.* Proceedings of the CSEE. 2003; 23(11): 139-144.
[10] Wenshao Bu, Shanming Wan, Shenghua Huang, et al. *General analytical model about controllable magnetic suspension force of bearingless motor.* Proceedings of the CSEE. 2009; 29(30): 84-89.
[11] Zhiquan Deng, Xiaolin Wang, Hongquan Zhang, et al. *nonlinear control of bearingless induction motors based on the motor rotor flux orientation*. Proceedings of the CSEE. 2003; 23(3): 89-92.
[12] Xinghua Zhang, Xianzhong Dai, Dajun Lu, Jianqiang Shen. A decoupling Control Method Based on Inverse System Theory foe Induction Motor Drives. *Electric Drive*. 2001; 2(5): 28-31.
[13] Jianrong Cao, Lie Yu, Youbai Xie. *Dynamic feedback linearization control for induction type bearingless motor.* Proceedings of the CSEE. 2001; 21(9): 22-26.
[14] Huangqiu Zhu, Tingting Zhang, Hualei Zou, Xiaoyan Diao. Decoupling control of bearingless synchronous reluctance motor based on inverse system method. *Chinese Control and Decision Conference.* Xuzhou. 2010; 1: 2120-2125.
[15] Qing Li, Xianxing Liu. *Decoupling control of the bearingless induction motor based on rotor flux orientation with inverse system theory.* International Conference on Measuring Technology and Mechatronics Automation. Shanghai. 2011; 1: 894-897.